Anal. Chem. **2000,** *72,* 5162−5171

Articles

A Kinetic Study of Mass Transfer in Reversed-Phase Liquid Chromatography on a C18-Silica Gel

Kanji Miyabe and Georges Guiochon*

Department of Chemistry, The University of Tennessee, Knoxville, Tennessee 37996-1600, and Division of Chemical and Analytical Sciences, Oak Ridge National Laboratory, Oak Ridge, Tennessee 37831

The characteristic features of mass-transfer kinetics in a reversed-phase (RP) column packed with a C18-silica were studied. The relevant information on phase equilibrium thermodynamics and mass-transfer kinetics was obtained by frontal analysis and the pulse method, respectively. The equilibrium isotherm was accounted for by the simple Langmuir model. The ratio of the axial dispersion coefficient to the mobile-phase flow velocity increased almost linearly with increasing solute concentration. Similarly, the mass-transfer rate coefficient (k_m) showed a linear dependence on the solute concentration. The positive concentration dependence of k_m resulted from that of the surface diffusion coefficient, which was interpreted with the chemical potential driving force model. The contribution of axial dispersion to band broadening was predominant in the RP column packed with the medium-size packing material used (particle diameter, 12 μm) whereas that of the kinetics of adsorption/desorption was negligibly small. The results of this study demonstrate how an analysis of the dependence of the mass-transfer kinetics on the flow velocity and the solute concentration allows a better understanding of this kinetics.

The positions and profiles of elution peaks in chromatography depend essentially on the thermodynamics of phase equilibrium, especially at high concentrations, in which range the asymmetry of the elution profile is strongly and foremost influenced by the curvature of the nonlinear equilibrium isotherm.[1] Numerous studies on separation mechanisms in chromatography have been made based on the use of the retention factor because of the major contribution of phase equilibrium under linear conditions on chromatographic behavior and of the high precision of retention factor data. The mass-transfer kinetics also influences peak profiles, particularly peak spreading and asymmetry.[1] However, in contrast with the large number of important studies on phase equilibrium and retention in chromatography, there are few fundamental studies on the characteristics of the mass-transfer kinetics in chromatography, especially on diffusion in packed beds and on the kinetics of adsorption/desorption at the adsorption sites. Detailed studies on the mass-transfer processes involved in columns provide essential information for the elucidation of the separation mechanisms in chromatography. The characteristic features of mass-transfer kinetics should be systematically analyzed in connection with phase equilibrium and the thermodynamic properties of chromatographic systems.

Previously, we reviewed surface diffusion data acquired in reversed-phase liquid chromatography (RPLC), under various experimental conditions (sample compounds, stationary and mobile phases).[2] It was concluded that the contribution of surface diffusion to intraparticle diffusion was important. We clarified some characteristics of surface diffusion in RPLC and derived a restricted molecular diffusion model as a first approximation for interpreting the intrinsic characteristics and the migration mechanism of surface diffusion.[2−4] Later, we advanced the quantitative analysis of the mass-transfer kinetics in different modes of chromatography, studying the anion-exchange chromatography of bovine serum albumin,[5,6] the enantiomeric separation of *S*-Tröger's base on cellulose triacetate[7] and that of phenyalanine anilide on an imprinted chiral stationary phase.[8,9] The analysis of the mass-transfer rate coefficients derived from breakthrough curves in the frontal analysis (FA) provided several kinetic parameters related to the four main mass-transfer processes taking place in a column:[1] (1) axial dispersion, (2) fluid-to-particle mass transfer, (3) intraparticle diffusion, and (4) adsorption/desorption kinetics. Further information was obtained on (1) the importance of the contributions of intraparticle diffusion (controlled, in some cases, by surface diffusion) and of the adsorption/desorption process to the kinetics of mass transfers in columns, (2) the concentration dependence of the mass-transfer rate coefficients, (3) the interpretation given by a heterogeneous surface model of

(1) Guiochon, G.; Shirazi, S. G.; Katti, A. M. *Fundamentals of Preparative and Nonlinear Chromatography*; Academic Press: Boston, MA, 1994.

(2) Miyabe, K.; Guiochon, G. *Adv. Chromatogr.* **2000**, *40*, 1.
(3) Miyabe, K.; Guiochon, G. *J. Phys. Chem. B* **1999**, *103*, 11086.
(4) Miyabe, K.; Guiochon, G. *Anal. Chem.* **2000**, *72*, 1475.
(5) Miyabe, K.; Guiochon, G. *Biotechnol. Prog.* **1999**, *15*, 740.
(6) Miyabe, K.; Guiochon, G. *J. Chromatogr., A* **2000**, *866*, 147.
(7) Miyabe, K.; Guiochon, G. *J. Chromatogr., A* **1999**, *849*, 445.
(8) Miyabe, K.; Guiochon, G. *Anal. Sci.* **2000**, *16*, 719.
(9) Miyabe, K.; Guiochon, G. *Biotechnol. Prog.* In press.

10.1021/ac0002801 CCC: $19.00
Published on Web 10/04/2000

the positive concentration dependence of the surface diffusion coefficient,[10,11] (4) the distribution of the adsorption energy on the surface of packing materials for anion-exchange chromatography and enantiomeric separations, and (5) the quantitative interpretation of the thermodynamic properties of the mass transfer in the chiral separation of *S*-Tröger's base.[7]

Most kinetic studies in chromatography so far were made by using various plate height equations.[1,12−18] Kinetic properties of the mass-transfer processes described above were analyzed on the basis of the different flow velocity dependences of the individual contributions of each process to the column efficiency. Much useful information on the mass-transfer kinetics was provided by a quantitative analysis of the correlation between the HETP (H) and the mobile-phase flow velocity (u) or between the reduced HETP (h) and the reduced velocity (ν). However, other approaches are available to obtain a more detailed knowledge of mass-transfer mechanisms in chromatography. A few physical parameters can be changed during a series of experiments without affecting the chemical properties of the separation system; besides the flow velocity of the mobile phase, they are the temperature, some physical properties of the packing material (particle diameter, internal porosity, micropore structure), the packing characteristics of the column bed (density and homogeneity), and the concentration of the compound studied. However, different columns must be used when the physical properties of the stationary-phase particles are changed, and in this case, it is difficult to prepare several columns having otherwise identical retention behavior and packing structure, even though the type of stationary phase is the same.[19] A change in the packing conditions of the column influences the contribution of axial dispersion to the column efficiency. So, changing the physical properties of the packing materials is not a tempting approach. On the other hand, the concentration of the compound and the temperature can be changed without causing any major change in the chemical properties of the separation system. Also, the influence of these two parameters on the chromatographic behavior are correlated with the phase equilibrium and the thermodynamic properties of the system, respectively. We analyzed previously[5−9] the concentration dependence of the rate coefficient to clarify the kinetic properties of the mass-transfer phenomena in a few modes of chromatography.

In the pulse on a plateau (PP) method,[1] pulse response experiments (elution chromatography) are made at different mobile-phase flow velocities and solute concentration. The PP method can simultaneously provide information on both the phase equilibrium and the mass-transfer kinetics.[20] This information is derived from an analysis of the elution profile of the peaks obtained as response to the injection of small samples on the plateaus achieved at different concentrations. The change in the height of the concentration step is correlated with the phase equilibrium. As in conventional studies of kinetics in linear chromatography, the information concerning the mass-transfer kinetics is obtained from an analysis of the dependence of H on u or of h on ν. It is the goal of this study quantitatively to analyze the kinetic properties of mass-transfer processes in RPLC columns, especially the intraparticle mass transfer in a column packed with C18-silica, and the adsorption/desorption process at the actual adsorption sites on this phase, and to demonstrate how the PP method can be used for a detailed investigation of mass-transfer kinetics in chromatographic columns.

THEORY

1. Phase Equilibrium. The experimental data on the phase equilibrium of the sample in RPLC was fitted to the simple Langmuir isotherm.[1]

$$q = q_s K_L C/(1 + K_L C) \tag{1}$$

where C and q are the concentrations of the solute in the mobile and the stationary phases, respectively, q_s is the saturation capacity and K_L the Langmuir parameter related to the adsorption energy. These two parameters were assumed to be independent of C.

2. Mass-Transfer Kinetics. Some equations derived for local linear isotherm conditions were used for the analysis of the profile of the elution peaks at different flow velocities on the plateaus achieved after the elution of the breakthrough curves corresponding to different concentration steps.

2.1. The Lumped Kinetic Model in Linear Chromatography. In the lumped kinetic model,[1] the overall mass-transfer rate in a column is correlated with two kinetic parameters, the axial dispersion coefficient (D_L) and the mass-transfer rate coefficient (k_m). The mass balance and the kinetic equations are as follows.

$$\frac{\partial C}{\partial t} + F\frac{\partial q}{\partial t} + u\frac{\partial C}{\partial z} = D_L\frac{\partial^2 C}{\partial z^2} \tag{2}$$

$$\partial q/\partial t = k_m(q^* - q) \tag{3}$$

where q^* is the concentration of the solute in the stationary phase in equilibrium with C, t the time, z the longitudinal distance along the column, u the average linear velocity of the mobile phase, and F the phase ratio ($F = (1 - \epsilon_T)/\epsilon_T$, with ϵ_T the total column porosity). The rate of mass transfer between stationary and mobile phases is given by eq 3 and is a function of k_m. The contributions to peak broadening of some mass-transfer processes, i.e., fluid-to-particle mass transfer, intraparticle diffusion, and adsorption/desorption kinetics, are lumped into k_m. Equation 3 assumes that the driving force of mass transfer is the difference between q^* and q and that the mass-transfer rate is proportional to the driving force. The following plate height equation for linear chromatography was derived by van Deemter et al.[13] from the analytical solution of eqs 2 and 3 proposed by Lapidus and Amundson.[21]

(10) Kapoor, A.; Yang, R. T.; Wong, C. *Catal. Rev.-Sci. Eng.* **1989**, *31*, 129.
(11) Suzuki, M. *Adsorption Engineering*; Kodansha/Elsevier: Tokyo, 1990.
(12) Giddings, J. C. *Dynamics of Chromatography*; Marcel Dekker: New York, 1965.
(13) van Deemter, J. J.; Zuiderweg, F. J.; Klinkenberg, A. *Chem. Eng. Sci.* **1956**, *5*, 271.
(14) Knox, J. H. *J. Chromatogr. Sci.* **1977**, *15*, 352.
(15) Knox, J. H. *Adv. Chromatogr.* **1998**, *38*, 1.
(16) Huber, J. F. K. *Ber. Bunsen-Ges. Phys. Chem.* **1973**, *77*, 179.
(17) Horváth, C.; Lin, H.-J. *J. Chromatogr.* **1976**, *126*, 401.
(18) Horváth, C.; Lin, H.-J. *J. Chromatogr.* **1978**, *149*, 43.
(19) Guiochon, G.; Farkas, T.; Guan-Sajonz, H.; Koh, J.-H.; Sarker, M.; Stanley B. J.; Yun, T. *J. Chromatogr., A* **1997**, *762*, 83.
(20) Sajonz, P.; Zhong, G.; Guiochon, G. *J. Chromatogr., A* **1996**, *731*, 1.
(21) Lapidus, L.; Amundson, N. R. *J. Phys. Chem.* **1952**, *56*, 984.

$$H = \frac{2D_L}{u} + 2\left(\frac{k'_0}{1+k'_0}\right)^2 \frac{u}{k'_0 k_m} \quad (4)$$

where k'_0 is the retention factor at infinite dilution. The following equation is obtained from the comparison of eq 4 with the plate height equation derived in the general kinetic model of chromatography[1].

$$\frac{F}{k'_0 k_m} = \frac{d_p}{6k_f} + \frac{{d_p}^2}{60D_e} + \left(\frac{k_p}{1+k_p}\right)^2 \frac{1}{k_{ads}} \quad (5)$$

with

$$k_p = \frac{1-\epsilon_p}{\epsilon_p} K_a \quad (5a)$$

where d_p is the particle diameter, k_f the external mass-transfer coefficient, D_e the intraparticle diffusivity, k_{ads} the adsorption rate constant, ϵ_p the internal porosity of the particle, and K_a the adsorption equilibrium constant. Equation 5 indicates how the mass-transfer rate coefficient in the solid-film linear driving force model (k_m) is related to the three kinetic parameters, i.e., the external mass transfer coefficient (k_f), the intraparticle diffusivity (D_e), and the adsorption rate constant (k_{ads}). The contributions of these three mass-transfer processes are additive. By combining eqs 4 and 5, the following HETP equation is derived for linear chromatography.[1]

$$H = \frac{2D_L}{u} + 2\left(\frac{k'_0}{1+k'_0}\right)^2 \left[\frac{ud_p}{6Fk_f} + \frac{u{d_p}^2}{60FD_e} + \left(\frac{k_p}{1+k_p}\right)^2 \frac{u}{Fk_{ads}}\right] \quad (6)$$

2.2. A HETP Equation in Local Linear Chromatography. The following equation can be used for analyzing the profile of elution peaks obtained under local linear isotherm conditions.

$$H = \frac{2D_L}{u} + 2\left(\frac{K}{1+K}\right)^2 \left[\frac{ud_p}{6Fk_f} + \frac{u{d_p}^2}{60FD_e} + \left(\frac{k_p}{1+k_p}\right)^2 \frac{u}{Fk_{ads}}\right] \quad (7)$$

where K is the partition coefficient in nonlinear chromatography ($= FK_a = F\,(\Delta q/\Delta C)$). Equation 7 is the same as eq 6, except that k'_0 is replaced by K. In this case, as in eq 5, k_m is the result of the combination of three kinetic parameters, k_f, D_e, and k_{ads}, through the following equation.

$$\frac{F}{Kk_m} = \frac{d_p}{6k_f} + \frac{{d_p}^2}{60D_e} + \left(\frac{k_p}{1+k_p}\right)^2 \frac{1}{k_{ads}} \quad (8)$$

The HETP under nonlinear conditions is a simple function of D_L and k_m, as follows.

$$H = \frac{2D_L}{u} + 2\left(\frac{K}{1+K}\right)^2 \frac{u}{Kk_m} \quad (9)$$

This equation is similar to eq 4 but it is valid for a pulse injected on a high-concentration plateau. This situation is called locally linear because, although the isotherm is nonlinear, when a small sample is injected the perturbation that it causes is linear.

2.3. Correlations for Some Kinetic Parameters. Equation 7 includes several kinetic parameters, D_L, k_f, D_e, and k_{ads}. The following equations were used to estimate some kinetic parameters related to D_L, k_f, and D_e. The axial dispersion is assumed to consist of two mechanisms,[1] molecular diffusion and fluid or eddy diffusion.

$$D_L = \gamma_1 D_m + \gamma_2 d_p u \quad (10)$$

where γ_1 and γ_2 are numerical parameters and D_m is the molecular diffusivity. Under the usual conditions of liquid chromatography, the contribution of molecular diffusion, the first term in the right-hand side of eq 10, to D_L is small compared with the second term.

The Wilson−Geankoplis equation was used to estimate k_f.[22]

$$Sh \equiv \frac{k_f d_p}{D_m} = \frac{1.09}{\epsilon} Sc^{1/3} Re^{1/3} \quad (0.015 < \mathrm{Re} < 55) \quad (11)$$

where Sh, Sc, and Re are the Sherwood, the Schmidt, and the Reynolds numbers, respectively, and ϵ is the interparticle void fraction of the column (external porosity). The value of D_m was estimated by the Wilke−Chang equation.[23,24]

$$D_m = 7.4 \times 10^{-8} \frac{(\alpha_{A,sv} M_{sv})^{1/2} T}{\eta_{sv} {V_{b,s}}^{0.6}} \quad (12)$$

where the subscripts s and sv denote the solute and the solvent, respectively, and α_A is the association coefficient, M the molecular weight, ç the viscosity, T the absolute temperature, and V_b the molar volume at normal boiling point.

The contributions of pore and surface diffusions to intraparticle diffusion were separated by assuming the parallel diffusion model.[11,25]

$$D_e = D_p + (1-\epsilon_p) K_a D_s \quad (13)$$

where D_p and D_s are the pore diffusivity and the surface diffusion coefficient, respectively. The value of D_p was calculated using the following equation.[1]

$$D_p = \left(\frac{\epsilon_p}{2-\epsilon_p}\right)^2 D_m \quad (14)$$

EXPERIMENTAL SECTION

Chemicals. All chemicals were used as supplied by their manufacturers. The stationary phase was Hyperprep HS BDS C18-silica gel (Shandon, Cheshire, England). HPLC grade methanol

(22) Wilson, E. J.; Geankoplis, C. J. *Ind. Eng. Chem. Fundam.* **1966**, *5*, 9.
(23) Reid, R. C.; Prausnitz, J. M.; Sherwood, T. K. *The Properties of Gases and Liquids*; McGraw-Hill: New York, 1977.
(24) Treybal, R. E. *Mass-Transfer Operations*; McGraw-Hill: New York, 1980.
(25) Ruthven, D. M. *Principles of Adsorption & Adsorption Processes*; Wiley: New York, 1984.

and water were from Fisher Scientific (Fairlawn, NJ). The sample compound, *p-tert*-butylphenol (PTBP), and the inert tracer, uracil, were from Aldrich (Milwaukee, WI). Another inert tracer, sodium nitrate, was from Mallinckrodt (Paris, KY).

Equipment. The instrument consisted in a Gilson piston pump model 302 (Gilson Medical Electronics, Middleton, WI), a Valco sampling valve (VICI, Houston, TX), and a Spectroflow 757 variable UV detector (Kratos, Ramsey, NJ). The detector was connected to an integrator for data acquisition, using a DOS-based software (Peaksimple II version. 3.54, SRI Instruments, Torrance, CA). The data acquired were downloaded to a computer of The University of Tennessee Computer Center for calculation of the moments of the peaks recorded.

Chromatographic Conditions. The C18-silica gel (d_p, 12 μm) was packed into a stainless steel tube (15 × 0.46 cm). The mobile phase was a (50:50, v/v) methanol/water mixture. The holdup and interparticle void volumes of the column were determined as 1.38 and 0.86 mL, respectively, by injecting uracil and sodium nitrate.[26] Under the conditions of this study, uracil was almost unretained. The total porosity (ϵ_T) of the column and the phase ratio (F) were 0.55 and 0.81, respectively. The bed interparticle void fraction (ϵ) and the intraparticle porosity (ϵ_p) of the packing material were 0.35 and 0.31, respectively. Chromatographic experiments were made at ambient temperature (297 ± 0.5 K). The experimental data measured with PTBP were recorded at wavelengths around 290 nm. In the PP method, the volumetric flow rate of the mobile phase (F_v) was changed in the range between 0.5 and 2.5 mL min^{-1}. The breakthrough curves in the single-step FA method were measured at F_v = 1.5 mL min^{-1}.

Procedures. First, the breakthrough curves of PTBP were recorded in the single-step FA mode, by replacing the pure mobile phase by a feed solution. The concentration of PTBP in the feed solutions was adjusted in the range between 1.0 × 10^{-3} and 1.0 × 10^{-2} g mL^{-1}. The equilibrium isotherm was derived from the experimental breakthrough curves using the area method. The isotherm data were fitted to the simple Langmuir model (eq 1).

Second, the pulse response experiments of PTBP were carried out at different surface coverages of the packing material, on the concentration plateau following a breakthrough curve. In the PP method, the difference between the concentrations of the perturbation pulse and the feed solution should be as small as possible. Each sample solution was prepared by dissolving a small additional amount of PTBP into the corresponding feed solution of the FA experiment. The difference in PTBP concentration between the sample solution and the feed solution pumped into the column was kept constant at 1.0 × 10^{-3} g mL^{-1}, because at high concentrations, the detector is not linear and its sensitivity is low. The injection volume of sample solution was 20 μL. The elution peaks on each concentration plateau were analyzed by assuming local linear isotherm conditions. The validity of this assumption was verified as described later.

RESULTS AND DISCUSSION

We first determined the equilibrium isotherm from the experimental breakthrough curves measured by single-step FA. Then, the elution peaks of the PP method were recorded at different heights of the concentration plateau and different flow velocities of the feed solution of PTBP. Kinetic parameters were estimated by analyzing the dependence of the column efficiency on the flow velocity and the concentration of PTBP. The characteristic features of the mass transfer in the C18-silica gel column and in the packing material were clarified from the analysis of these kinetic parameters.

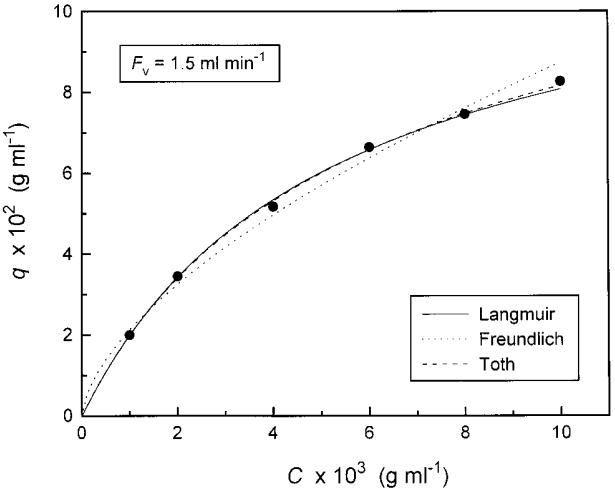

Figure 1. Representation of the phase equilibrium of PTBP by the Langmuir, Toth, and Freundlich models.

1. Determination of Phase Equilibrium. Figure 1 shows the correlation of the phase equilibrium, a plot of the experimental data determined by FA at F_v = 1.5 mL min^{-1} (the intermediate flow rate in the range used for the PP method). The symbols show the experimental data. These data fit well to the simple Langmuir isotherm (eq 1, Figure 1, solid line). The best parameters are q_s = 0.122 g mL^{-1} and K_L = 195 mL g^{-1}. The data fit well also to the Toth equation[1] (Figure 1, dashed line),

$$q = abC/(b^{t'} + C^{t'})^{1/t'} \qquad (15)$$

The best parameters for this model are a = 24.7, b = 5.4 × 10^{-3} mL g^{-1}, and t' = 0.91. The value of t' is close to unity, suggesting that the Langmuir isotherm is as appropriate. These results are consistent with previous observations that phase equilibria in RPLC systems using C18-silica gels are usually well represented by the simple Langmuir model.[1] As illustrated in Figure 1, the amount adsorbed (q) is 8.3 × 10^{-2} g mL^{-1} at C = 1.0 × 10^{-2} g mL^{-1}. In this study, surface coverage ($\theta = q/q_s$) was varied between 0 and ~0.68. This is sufficient for an accurate estimate of the saturation capacity.

Figure 1 shows also the best fit of the data to the Freundlich isotherm (dotted line). This isotherm was not used because the calculated isotherm does not agree with the experimental data and the model is thermodynamically inconsistent.[1,11]

2. Confirmation of Local Linear Isotherm Conditions. In the PP method, the difference between the concentrations of the perturbation pulse and the feed solution should be as small as possible. As explained earlier, this difference (ΔC) had to be kept equal to 1.0 × 10^{-3} g mL^{-1} because the sensitivity of the detector at high concentrations is low. So, it is necessary to verify the validity of the assumption of a local linear behavior during the experimental procedure in the PP method.

(26) Wells, M. J. M.; Clark, C. R. *Anal. Chem.* **1981**, *53*, 1431.

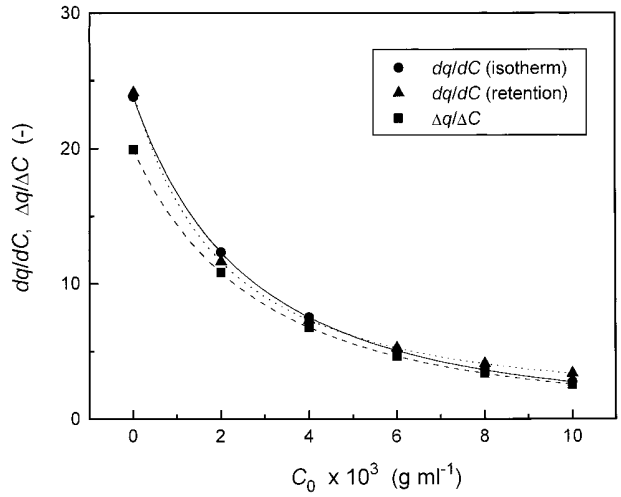

Figure 2. Comparison of the slope of the tangent of the equilibrium isotherm (dq/dC) with both the slope of the isotherm chord ($\Delta q/\Delta C$) and dq/dC calculated from the retention of the elution peak in the method of a pulse on a plateau.

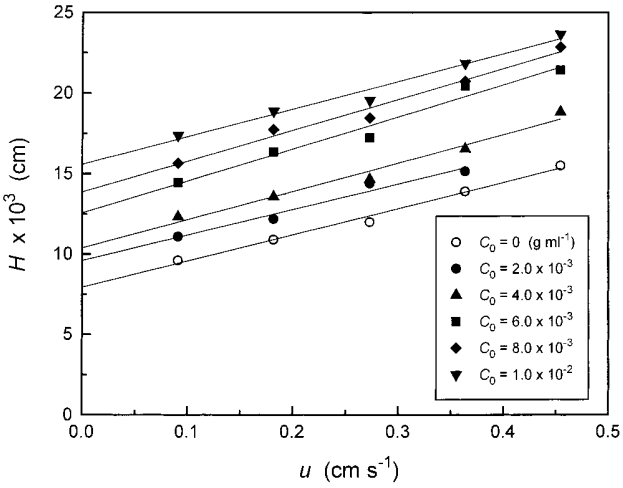

Figure 3. Dependence of the HETP on the flow velocity of the feed solution or mobile phase.

Figure 2 compares the slopes of the tangent and the chord of the Langmuir isotherm (Figure 1). The solid circles represent the slope of the tangent of the isotherm (dq/dC) at each concentration of PTBP in the feed solutions, as calculated from

$$\mathrm{d}q/\mathrm{d}C = q_s K_L/(1 + K_L C)^2 \qquad (16)$$

The solid squares represent the slope of the isotherm chord ($\Delta q/\Delta C$) corresponding to $\Delta C = 1.0 \times 10^{-3}$ g mL^{-1}. There is a small difference between dq/dC and $\Delta q/\Delta C$ at low concentrations but it decreases with increasing C_0. The values of dq/dC and $\Delta q/\Delta C$ are almost identical at high concentrations. The solid triangles show the apparent value of dq/dC calculated from the retention of the perturbation peaks. Even at low concentrations, the two estimates of the slopes of the tangents, calculated from the equilibrium isotherm (solid circle) and from the retention data (solid triangle), are almost the same. The difference between dq/dC calculated from the retention data and the slope of the isotherm chord ($\Delta q/\Delta C$) is due to the dilution of the perturbation taking place during the chromatographic process. The results in Figure 2 show that the measurements of the perturbations of the concentration plateaus in the PP method were done under locally linear conditions.

3. Estimation of Kinetic Parameters. The kinetic parameters in eq 7, D_L, D_e, D_s, and k_{ads}, were estimated as follows.

3.1. Estimation of D_L. As described in eq 10, it is usually assumed that axial dispersion results from two different mechanisms, axial molecular diffusion and fluid flow dispersion or eddy diffusion.[1] The contribution of axial molecular diffusion to axial dispersion is negligible at the flow rates used in this study. Thus, the first term in the RHS of eq 9 is independent of u. The kinetic parameters, D_L and k_m, can be calculated separately by taking advantage of the difference in the flow velocity dependence of the two terms in the RHS of eq 9. We assumed here that k_m is independent of u. Only the first term of the RHS of eq 8, $d_p/(6k_f)$, depends on u, through k_f. As shown in eq 11, k_f is assumed to be proportional to the power $^1/_3$ of u. Under our experimental conditions, the contribution of $d_p/(6k_f)$ to $F/(Kk_m)$ is ~1.7 ($= 5^{1/3}$) times larger at $F_v = 0.5$ mL min^{-1} than at 2.5 mL min^{-1}. Thus, the assumption that k_m does not depend on u has little influence on our results because of the small contribution of the first term, $d_p/(6k_f)$, to $F/(Kk_m)$, as described later.

Figure 3 illustrates the experimental correlation observed between H and u at different concentrations. Although the data are slightly scattered, nearly linear correlations are observed. At $C_0 = 0$, the intercept is 7.9×10^{-3} cm. The corresponding HETP (h) is 6.6, a value somewhat larger than usual for a well-packed column. The slope at $C_0 = 0$ is 1.6×10^{-2} s, from which the slope of the linear correlation between h and the reduced velocity (ν) is calculated (4.6×10^{-2}), suggesting that the mass-transfer properties in the particles used here are ordinary and close to average. However, the experimental data in Figure 3 are in agreement with eq 9 only if we assume that the ratio D_L/u in this equation is constant or nearly so. The kinetic parameters D_L/u and k_m were respectively estimated from the intercept and the slope of the linear correlations in Figure 3 (see eq 9).

Figure 4 shows a plot of these values of D_L/u derived from the data in Figure 3 versus the feed concentration. They increase almost linearly with increasing C_0. Using the random-walk model, Giddings[12] made a detailed analysis of the influence of different mass-transfer processes on the axial peak dispersion. He suggested that fluctuations of the flow velocity across the bulk mobile-phase stream take place on different scales and distinguished the *trans-channel*, *short-range interchannel*, *long-range interchannel*, and *trans-column* contributions. He derived the following equation for the contributions of eddy diffusion and stream splitting to band broadening from the coupling theory.[12]

$$H = \sum \frac{1}{1/2\lambda_i d_p + D_m/\omega_i u d_p^2} \qquad (17)$$

where λ and ω are geometrical parameters. Equation 17 indicates that H approaches a constant value, $2\lambda d_p$ (stream-splitting mechanism), at high flow velocities. By contrast, at low velocities, H approaches the value, $\omega u d_p 2/D_m$ (diffusive mechanism) and is

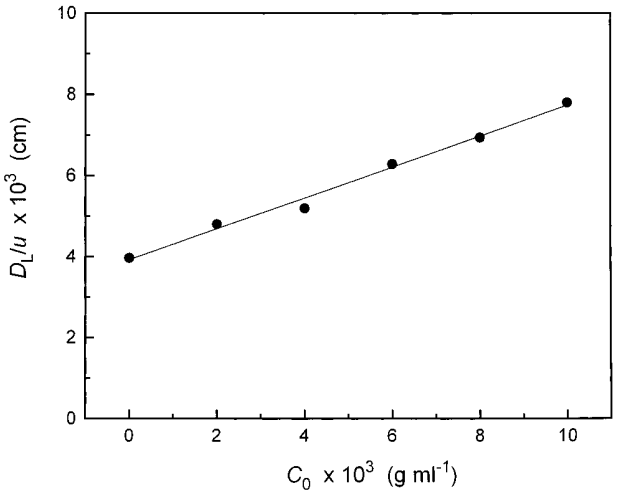

Figure 4. Concentration dependence of D_L/u.

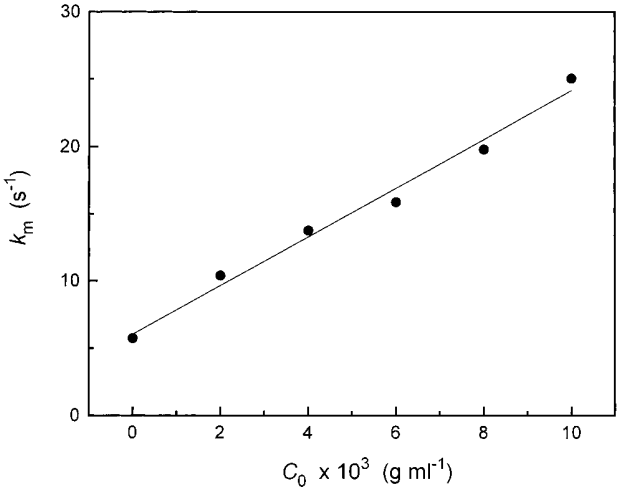

Figure 5. Concentration dependence of k_m.

proportional to u. Quantitative analysis of the individual contributions of each stream splitting to band broadening indicates that the contributions of the *trans-channel* and *trans-column* fluctuations are dominant and that they depend mainly on $D_m/(\omega u d_p 2)$ in the flow rate range used in this study (reduced velocities, $\nu = 26 - 132$).[12] Most literature correlations used to estimate D_m are based on the assumption that D_m is inversely proportional to the viscosity (η), although it is suggested that D_m is proportional to $\eta^{-0.5} - \eta^{-1}$ in a wide range of η.[23] Furthermore, the viscosity of a solution increases almost linearly with increasing solute concentration at low concentrations.[1] Thus, it is likely that the increase in viscosity of the feed solution of PTBP is the main cause of the positive concentration dependence of D_L/u shown in Figure 4.

This study provides the first demonstration of a linear increase of the ratio D_L/u with increasing solute concentration. It also provides an explanation of this linear dependence on the basis of an equation (eq 17) that was first derived by Giddings.[12]

3.2. Estimation of k_{ads}. Figure 5 shows the concentration dependence of k_m, derived from the slope of the linear correlations in Figure 3. As for D_L/u, an almost linear correlation is observed. Many publications have reported a concentration dependence of the rate parameters and/or the diffusivities, for example, for k_m and for the lumped mass-transfer rate coefficient ($k_{m,L}$), in various

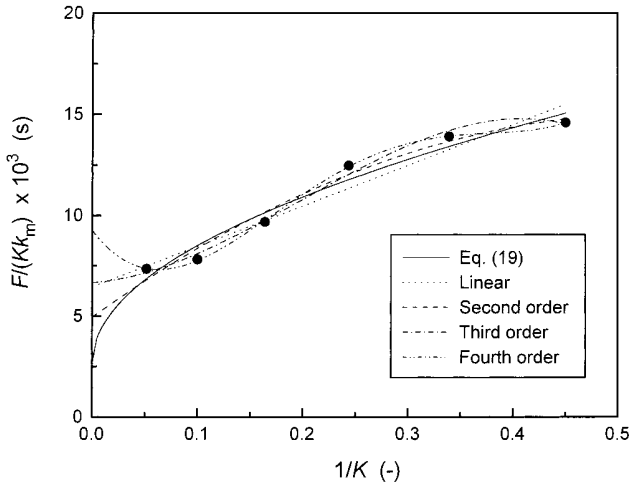

Figure 6. Correlation between $F/(Kk_m)$ with $1/K$.

separation or liquid-phase systems.[2,27−37] The tendency of k_m and $k_{m,L}$ to increase with increasing solute concentration seems general. We show later that information on the kinetics of adsorption/desorption at the actual adsorption sites on the packing material can be derived from a quantitative analysis of the concentration dependence of k_m.

Equation 8 suggests that $F/(Kk_m)$ tends toward the sum of the following two terms, $(d_p/6k_f)$ and $(1/k_{ads})$, when K increases indefinitely. Even when the contribution of surface diffusion to intraparticle diffusion cannot be neglected compared with that of pore diffusion in eq 13, the second term in the RHS of eq 8, $d_p^2/(60D_e)$, becomes probably negligible because D_e increases also with increasing K (eq 13). The coefficient of $(1/k_{ads})$ in eq 8, $(k_p/(1 + k_p))^2$, tends toward unity when $K = 4$. In conclusion, k_{ads} could be estimated from the value of $F/(Kk_m)$ at $1/K = 0$ because k_f can be estimated with a reasonable accuracy, using conventional literature correlations.

In Figure 6, the experimental values of $F/(Kk_m)$ are plotted against $1/K$. $F/(Kk_m)$ increases with decreasing K. This variation arises from that of the second term in the RHS of eq 8, $d_p 2/(60D_e)$. We assume in this work that k_f and k_{ads} are independent of the concentration of PTBP and of K. This assumption has little influence on the conclusions of this study because the contributions to peak spreading of the two corresponding mass-transfer processes, the fluid-to-particle mass transfer and the adsorption/desorption, are small (see later). Taking into account the results of this study, the second term, $d_p 2/(60D_e)$, can be rewritten to ex-

(27) Guan-Sajonz, H.; Sajonz, P.; Zhong, G.; Guiochon, G. *Biotechnol. Prog.* **1996**, *12*, 380.
(28) Sajonz, P.; Guan-Sajonz, H.; Zhong, G.; Guiochon, G. *Biotechnol. Prog.* **1997**, *13*, 170.
(29) Seidel-Morgenstern, A.; Jacobson, S. C.; Guiochon, G. *J. Chromatogr.* **1993**, *637*, 19.
(30) Rearden, P.; Sajonz, P.; Guiochon, G. *J. Chromatogr., A* **1998**, *813*, 1.
(31) Sajonz, P.; Kele, M.; Zhong, G.; Sellergren, B.; Guiochon, G. *J. Chromatogr., A* **1998**, *810*, 1.
(32) Al-Duri, B.; McKay, G. *J. Chem. Tech. Biotechnol.* **1992**, *55*, 245.
(33) Gibbs, S. J.; Chu, A. S.; Lightfoot, E. N.; Root, T. W. *J. Phys. Chem.* **1991**, *95*, 467.
(34) Lederer, K.; Amtmann, I.; Vijayakumar, S.; Billiani, J. *J. Liq. Chromatogr.* **1990**, *13*, 1849.
(35) Gallagher, W. H.; Woodward, C. K. *Biopolymer* **1989**, *28*, 2001.
(36) Marlowe, R. L.; Jackson, H. E. *Spectrosc. Lett.* **1990**, *23*, 1203.
(37) Friedrich, M.; Seidel, A.; Gelbin, D. *Chem. Eng. Process* **1998**, *24*, 33.

press that (1) the phase equilibrium is accounted for by the simple Langmuir isotherm (eq 1), (2) the contribution of surface diffusion to intraparticle diffusion is significantly larger than that of pore diffusion (see later), and (3) the positive concentration dependence of the surface diffusion coefficient (D_s) is probably best interpreted by the chemical potential driving force model (see later).

$$\frac{d_p^2}{60D_e} \approx \frac{Fd_p^2}{60(1-\epsilon_p)D_{s,0}(q_sK_L)^{1/2}K^{1/2}} \qquad (18)$$

where $D_{s,0}$ is D_s at $q = 0$. By using eq 18, eq 8 can be rewritten as follows.

$$\frac{F}{Kk_m} \approx \frac{d_p}{6k_f} + \frac{Fd_p^2}{60(1-\epsilon_p)D_{s,0}(q_sK_L)^{1/2}K^{1/2}} + \left(\frac{k_p}{1+k_p}\right)^2\frac{1}{k_{ads}} \qquad (19)$$

Equation 19 implies that $F/(Kk_m)$ is proportional to $(1/K)^2$. Although the third term in the RHS of eq 19 depends also on K, the concentration dependence of $(k_p/(1 + k_p))^2(1/k_{ads})$ can be neglected because of the small contribution of this term to $F/(Kk_m)$ (see later). The solid line in Figure 6 is calculated according to eq 19. It accounts well for the experimental data (symbols).

Figure 6 also illustrates four polynomial regressions to correlate $F/(Kk_m)$ and $1/K$. The second-order regression provides a profile similar to the one based on eq 19. The other three types of regression give quite different profiles at low values of $1/K$. The intercept of $F/(Kk_m)$ at $1/K = 0$ is estimated as 2.7×10^{-3} and 4.9×10^{-3} s from the solid (eq 19) and the dashed (second-order regression) line intercepts, respectively. With 2.7 ms as the intercept, however, we obtain $k_{ads} = -970$ s^{-1} because the value of $d_p/6k_f$ is estimated at 3.7×10^{-3} s. Although a negative value of k_{ads} is unreasonable, this result probably suggests that the contribution of the kinetics of the adsorption/desorption process to band broadening is negligibly small in RPLC. The intercept derived from the second-order regression gives $F/(Kk_m) = 4.9 \times 10^{-3}$ s at $1/K = 0$ leading to $k_{ads} = 800$ s^{-1}.

In previous reports,[5−8] we derived k_{ads} through a similar analysis of the concentration dependence of k_m or $k_{m,L}$ in various modes of chromatography. The following values of k_{ads} were obtained: 1 to 30 s^{-1} for bovine serum albumin in anion-exchange chromatography,[5,6] ∼0.5 s^{-1} for the *S* enantiomer of Tröger's base on cellulose triacetate,[7] and ∼50−90 s^{-1} for L- and D-phenylalanine anilide on a polymeric imprinted chiral stationary phase.[8] It is likely that the kinetics of adsorption/desorption is faster in RPLC than on the other separation systems. Although we found no value of k_{ads} in RPLC, the adsorption rate constants of low molecular weight hydrocarbons (ethane, propane, butane) on a silica gel were reported to be of the order of 100−1000 s^{-1},[38] roughly of the same order of magnitude as those determined in this study. In conclusion, the contribution of the adsorption/desorption kinetics to band broadening is negligibly small in RPLC.

As indicated above, this work provides the first estimate of k_{ads} for a RPLC system. To the best of our knowledge, there is no other value of k_{ads} in the literature to which we could compare our result. The value obtained supports the conventional assumption that the kinetics of adsorption/desorption on the actual adsorption sites of the stationary phase contribute little to band broadening in RPLC. Obviously, the acquisition of numerous values of k_{ads} under various separation conditions, in different modes of chromatography, is required for an improved understanding of this issue.

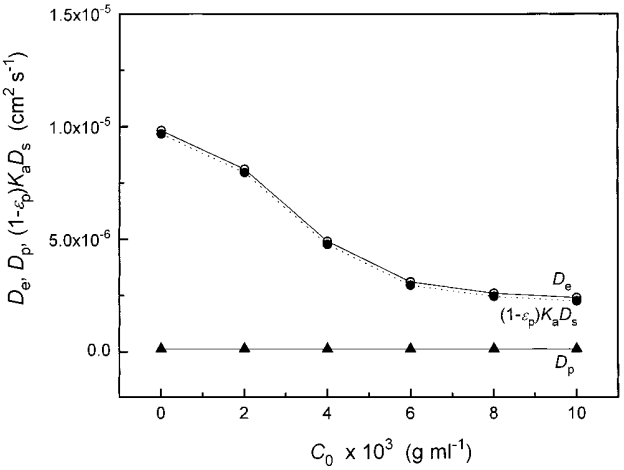

Figure 7. Comparison of the contributions of the pore and surface diffusions to the intraparticle diffusion.

3.3. Estimation of D_e and D_s. The intraparticle dispersion, D_e, can now be derived from k_f (eq 11) and k_{ads} (section above), using eq 8. Figure 7 shows that D_e decreases with increasing C_0. Figure 7 shows also plots of the contributions of pore and surface diffusion to the intraparticle diffusion of PTBP as functions of C_0. The difference between D_e (open circle) and D_p (pore diffusion, solid triangle) corresponds to the contribution of surface diffusion (solid circle). Obviously, the contribution of surface diffusion is much larger than that of pore diffusion. The value of D_p was derived from eq 14; its concentration dependence was neglected. Because of the small contribution of pore diffusion to intraparticle diffusion, the limited accuracy in the estimation of D_p and the error made in assuming that D_p (and D_m) do not depend on the solute concentration have little influence on our results.

Like D_e, the contribution of surface diffusion to intraparticle diffusion decreases with increasing C_0 (Figure 7). This relationship is explained by the concentration dependence of K_a and D_s, cf eq 13. Figure 2 shows the correlation between dq/dC ($= K_a = K/F$) and C_0. The decrease of K_a when C_0 increases from 0 to 1×10^{-2} g mL^{-1} is larger than that of the contribution of surface diffusion to intraparticle diffusion (Figure 7, solid circles), which suggests that D_s increases with increasing C_0. A similar positive concentration dependence of D_s was reported in various liquid chromatographic systems[2,5,6,8,9] and in other gas- and liquid-phase adsorption systems.[10,11] The results in Figures 2 and 7 indicate that the positive concentration dependence of k_m illustrated in Figure 5 results from that of D_s.

The concentration dependence of D_s could be explained by the chemical potential driving force model,[10,11,25] in which D_s is given by

$$D_s = D_{s,0}((\mathrm{d}\ln C)/(\mathrm{d}\ln q)) \qquad (20)$$

where $D_{s,0}$ is the value of D_s at $q = 0$. The value of $(\mathrm{d}\ln C)/(\mathrm{d}\ln$

(38) Schneider, P.; Smith, J. M. *AIChE J.* **1968**, *14*, 762.

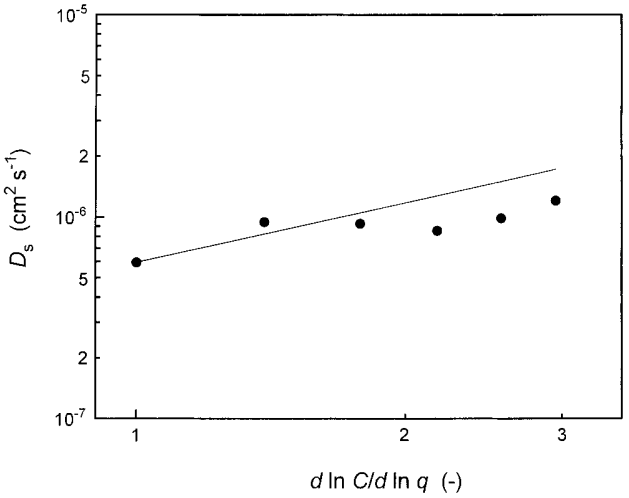

Figure 8. Logarithmic plot of D_s against d ln C/d ln q.

q) is the slope of the equilibrium isotherm in a double-logarithmic plot. It is equal to $1 + K_L C$ when the phase equilibrium is accounted for by the Langmuir isotherm (eq 1). The logarithm of the experimental values of D_s are plotted against (d ln C)/(d ln q) in Figure 8 where the solid line shows the linear correlation between ln D_s and ln(d ln C/d ln q) having a slope unity and passing through $D_{s,0}$ at $q = 0$. Although the plot in Figure 8 has a somewhat winding profile, the agreement is good and it is likely that the concentration dependence of D_s is explained by the chemical potential driving force model. In a previous paper,[2] we reported that the concentration dependence of D_s for *p-tert*-octylphenol in a RPLC system using a C18-silica gel could also be interpreted by the chemical potential driving force model.

In Figure 8, D_s for PTBP is of the order of $\sim 1 \times 10^{-7}$–1×10^{-6} cm^2 s^{-1}. Although the value of D_s is influenced by the physical and chemical properties of the compound studied, the stationary and the mobile phases used in the separation system, some literature data of D_s in RPLC previously presented are cited for the sake of comparison. In previous papers,[2–4,39] we studied surface diffusion phenomena in RPLC, changing the compounds and the stationary and the mobile phases. Values of D_s between 1×10^{-7} and 1×10^{-5} cm^2 s^{-1} were reported under common RPLC conditions. It was also found that D_s was 1–2 orders of magnitude smaller than the corresponding D_m. Table 1 lists other experimental data reported on surface and lateral diffusions in RPLC.[40–43] These results show the validity of the estimate of D_s made in this study.

This work demonstrates also that, in RPLC as in other liquid-phase systems,[2,27–37] k_m increases with increasing solute concentration. It shows for the first time that the linear positive dependence of k_m on the solute concentration results from a similar concentration dependence of D_s. Finally, it suggests that the dependence of D_s on the solute concentration could be interpreted in terms of the chemical potential driving force model.

(39) Miyabe, K.; Guiochon, G. *Anal. Chem.* **1999**, *71*, 889.
(40) Bogar, R. G.; Thomas, J. C.; Callis, J. B. *Anal. Chem.* **1984**, *56*, 1080.
(41) Wong, A. L.; Harris, J. M. *J. Phys. Chem.* **1991**, *95*, 5895.
(42) Zulli, S. L.; Kovaleski, J. M.; Zhu, X. R.; Harris, J. M.; Wirth, M. J. *Anal. Chem.* **1994**, *66*, 1708.
(43) Hansen, R. L.; Harris, J. M. *Anal. Chem.* **1995**, *67*, 492.

Table 1. Surface and Lateral Diffusion Data in RPLC

solute	stationary phase	mobile phase	temp (K)	D_s[a] (cm^2 s^{-1})	ref
pyrene	C18	methanol/water (75/25, v/v)	*b*	2.5×10^{-7}	40
iodine	C1	methanol/water (50/50, v/v)	*b*	3.9×10^{-8}	41
iodine	C1	methanol/water (75/25, v/v)	*b*	7.2×10^{-8}	41
acridine orange	C18	water	293	1.3×10^{-7}	42
rubrene	C18	water	*b*	1.5×10^{-9}	43
rubrene	C18	methanol/water (10/90, v/v)	*b*	2.1×10^{-9}	43
rubrene	C18	methanol/water (20/80, v/v)	*b*	2.8×10^{-9}	43

[a] D_s represents both surface and lateral diffusion coefficients. [b] No information about temperature was indicated in the references.

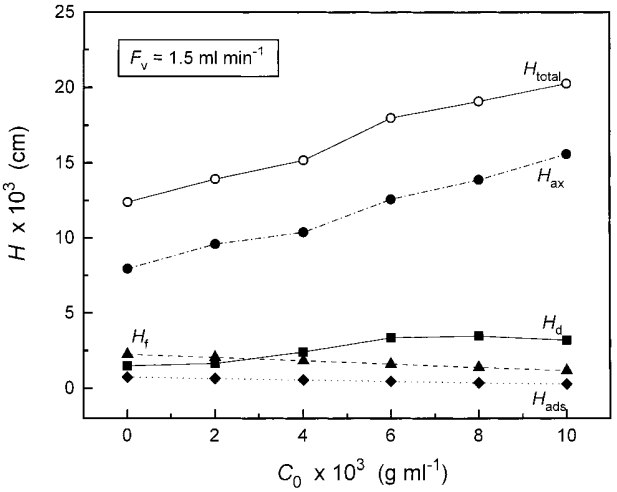

Figure 9. Comparison of the contributions of the mass-transfer resistances of each kinetic process in the C18-silica gel column to the overall efficiency at different PTBP concentrations. HETP: H_{total}, overall column efficiency; H_{ax}, axial dispersion; H_f, fluid-to-particle mass transfer; H_d, intraparticle diffusion; and H_{ads}, adsorption/desorption.

These results are important because, despite the important contribution of surface diffusion to intraparticle diffusion illustrated in Figure 7, the significance of surface diffusion is not yet recognized in kinetic studies of chromatography. This study demonstrates the predominant role of surface diffusion in the mass-transfer kinetics in RPLC through its influence on k_m. The characteristics of surface diffusion and its role in the mass-transfer mechanisms are subjects of intense current interest in chromatography and in chemical engineering.[3]

4. Comparison of the Contributions of the Four Mass-Transfer Processes to the HETP of PTBP. Equation 7 correlates the total HETP (H_{total}) with the different kinetic parameters identified, D_L, k_f, D_e (D_p and D_s), and k_{ads}. The values of these parameters were obtained as described above, at different PTBP concentrations. The contributions of the four terms in the RHS of eq 7 to H_{total} can now be calculated and compared. Figure 9 shows the results of these calculations. The contribution of axial dispersion (H_{ax}) is dominant. It varies from about 64 to 77%, depending on the PTBP concentration. The contribution of the adsorption/desorption kinetics (H_{ads}) is small ($\sim$1.4–5.9%). The

contributions of the fluid-to-particle mass transfer (H_f) and of intraparticle diffusion (H_d) are about 5.8−18% and 12−19%, respectively, which is rather moderate.

In this work, we used a column packed with an intermediate-size packing material. As explained earlier, the quality of the packed bed was not quite satisfactory and this the main reason for the large contribution of H_{ax} to H_{total} in Figure 9. As indicated in eqs 7 and 10, the magnitude of the contribution of H_{ax} to H_{total} depends linearly on d_p. Similarly, those of H_f and H_d are proportional to the five-thirds and the second power of d_p, respectively. On the other hand, the contributions of H_d and H_{ads} to H_{total} are linearly proportional to u, whereas that of H_{ax} is independent of u and that of H_f is proportional to the two-thirds power of u Equation 7 suggests that the contributions of the three mass-transfer processes to band broadening other than the axial dispersion, and especially that of H_d, increase with increasing d_p or u. Under different experimental conditions, for instance, in preparative chromatography using large packing materials and a high flow velocity, different results would be observed and the fractional contributions of each mass-transfer process to H_{total} could be markedly changed. The results of this study suggest that the contributions of H_{ax} to H_{total} would be large in a conventional RP column packed with relatively small packing materials. A more detailed study on the axial dispersion process is necessary to clarify the characteristics of the mass-transfer kinetics involved in RP columns used for analytical purpose.

CONCLUSION

In conclusion, the pulse on a plateau method proved useful for the determination of the kinetic parameters of the mass-transfer processes in a chromatographic column, in addition to its more conventional application to the determination of equilibrium isotherms. This information was derived from the analysis of the dependence of the HETP on the mobile-phase velocity and of the mass-transfer rate coefficient, k_m, on the solute concentration. Both the axial dispersion coefficient, D_L, and k_m increase with increasing C_0. This work provides the first demonstration of the linear increase of the ratio D_L/u with increasing solute concentration. Equation 17 suggests that the main cause for the concentration dependence of D_L is probably the increase of the viscosity of the feed solution percolating through the column during the FA and PP measurements. The concentration dependence of k_m results from that of the intraparticle diffusivity, D_e, itself explained by that of the surface diffusion, D_s. Our work demonstrates also for the first time that the linear dependence of k_m on C_0 stems from the similar concentration dependence of D_s. Surface diffusion gives the dominant contribution to intraparticle diffusion. The positive concentration dependence of D_s was interpreted satisfactorily by the chemical potential driving force model.

Although a definitive value of k_{ads} could not be accurately determined in this study because the corresponding HETP contribution is small, it was shown that k_{ads} is large in RPLC, much larger than in most other modes of chromatography. This result proves the validity of the assumption made in previous studies on the mass-transfer kinetics in RPLC that the contribution to band broadening of the adsorption/desorption kinetics at the actual adsorption sites is negligible compared to those due to other mass-transfer processes. Finally, we provided the first estimate of k_{ads} in a RPLC system. More similar investigations leading to the determination of k_{ads} under various experimental conditions, in different modes of chromatography are required to further elucidate the relative importance of this step. For the column used in this study, the contribution of axial dispersion was larger than those of the other three mass-transfer processes combined. This suggests that more detailed studies of axial dispersion are required to elucidate the kinetics of mass transfer in analytical RP columns.

ACKNOWLEDGMENT

This work was supported in part by Grant CHE-97-01680 of the National Science Foundation and by the cooperative agreement between the University of Tennessee and the Oak Ridge National Laboratory.

LIST OF SYMBOLS

a	parameter of the Toth isotherm (−)
b	parameter of the Toth isotherm (g mL^{-1})
C	concentration of the solute in the mobile phase (g mL^{-1})
ΔC	increment of the concentration step (g mL^{-1})
C_{inj}	concentration of the solute in the sample solution (g mL^{-1})
C_0	concentration of the solute in the feed solution (g mL^{-1})
d_p	particle diameter (cm)
D_e	intraparticle diffusivity (cm^2 s^{-1})
D_L	axial dispersion coefficient (cm^2 s^{-1})
D_m	molecular diffusivity (cm^2 s^{-1})
D_p	pore diffusivity (cm^2 s^{-1})
D_s	surface diffusion coefficient (cm^2 s^{-1})
$D_{s,0}$	D_s at zero surface coverage (cm^2 s^{-1})
F	phase ratio (= $(1 - \text{å}_T)/\text{å}_T$) (−)
F_v	volumetric flow rate of the feed solution and mobile phase (mL min^{-1})
h	reduced plate height (−)
H	height equivalent to a theoretical plate (cm)
k_{ads}	adsorption rate constant (s^{-1})
k_f	external mass-transfer coefficient (cm s^{-1})
k_m	mass-transfer rate coefficient representing the contributions of the fluid-to-particle mass transfer, the intraparticle diffusion, and the adsorption/desorption to band broadening (s^{-1})
$k_{m,L}$	lumped mass-transfer rate coefficient representing the contributions of the axial dispersion, the fluid-to-particle mass transfer, the intraparticle diffusion, and the adsorption/desorption to band broadening (s^{-1})
k_p	defined in eq 5a (−)
k_0'	retention factor at infinite dilution (−)
K	partition coefficient in nonlinear chromatography (= $FK_a = F(\Delta q/\Delta C)$) (−)
K_a	adsorption equilibrium constant (−)
K_L	parameter of the Langmuir isotherm (mL g^{-1})
M	molecular weight (−)

q	concentration of the solute in the stationary phase (g mL^{-1})
q_s	saturated amount adsorbed (g mL^{-1})
q^*	q in equilibrium with C (g mL^{-1})
dq/dC	slope of the tangent of the equilibrium isotherm (−)
$\Delta q/\Delta C$	slope of the isotherm chord (−)
Re	Reynolds number (−)
Sc	Schmidt number (−)
Sh	Sherwood number (−)
t	time (s)
t'	parameter of the Toth isotherm (−)
T	absolute temperature (K)
u	average velocity of the feed solution and mobile phase (cm s^{-1})
V_b	molar volume at the normal boiling point (cm^3 mol^{-1})
z	longitudinal distance along the column (cm)

Greek Symbols

α_A	association coefficient (−)
γ_1	parameter in eq 10 (−)
γ_2	parameter in eq 10 (−)
ϵ	void fraction of the column (−)
ϵ_p	intraparticle porosity (−)
ϵ_T	total porosity of the column (−)
η	viscosity (Pa s)
θ	surface coverage (−)
λ	geometrical parameter in eq 17 (−)
ν	reduced flow velocity (−)
ω	geometrical parameter in eq 17 (−)

Subscripts

ads	contribution of adsorption/desorption
ax	contribution of axial dispersion
d	contribution of intraparticle diffusion
f	contribution of fluid-to-particle mass transfer
I	each flow velocity fluctuation
s	solute
sv	solvent
total	overall column

Received for review March 9, 2000. Accepted August 22, 2000.

AC0002801